ARTICLES

Preparation and Spectroscopic Characterization of $[Pt(en)_2I_2][Pt(CN)_4]$: A New Quasi-One-Dimensional Mixed Valence Chain Material in a Completely Ordered Lattice

James A. Brozik,*,† Brian L. Scott,‡ and Basil I. Swanson*,‡

Department of Chemistry, The University of New Mexico, Albuquerque, New Mexico 87131, and Chemical Science and Technology Division, Los Alamos National Laboratory, Los Alamos, New Mexico 87545

Received: February 8, 1999; In Final Form: September 5, 1999

The unique linear chain compound $[Pt(en)_2I_2][Pt(CN)_4]$ {where en = ethylenediamine} has been synthesized through a standard method. The results of a structural analysis by X-ray crystallography reveal this new MX compound to be quasi-one-dimensional with complete chain-to-chain registry to give a completely ordered structure. The results of resonance Raman, IR, diffuse reflectance, and X-ray crystallography reveal that the Pt centers are highly charge disproportionated with a large commensurate distortion of the iodide sublattice about the Pt center of higher charge. These results reveal that this material is the strongest CDW MX compound, containing iodide bridges, reported to date. Resonance Raman experiments have shown that five A_g (C_{2h} site symmetry) Raman bands are strongly enhanced. These correspond to three in-chain Pt-I modes and two (chain perpendicular) CN stretches and are interpreted in terms of strong phonon coupling to the IVCT band.

Introduction

Halogen bridged transition metal chain compounds (MX) have become an important class of materials in the study of a wide variety of broken symmetry ground and excited states which are unique to one-dimensional materials.[1] The one-dimensional structures of MX materials can be described as a linear chain with the sequence $-M^{2+}-X^{-}-M^{4+}-X^{-}-$ (where M = Pt, Pd, or Ni and X = Cl, Br, or I). These materials typically display a commensurate charge disproportionation of the metal sublattice (charge density wave or CDW) accompanied by a Peierls distortion of the halide sublattice about the transition metal of higher charge. Earlier studies have demonstrated that the CDW nature of these materials can be systematically tuned by simple chemical modification, pressure changes, and chemical doping to yield materials that are dominated by strong electron−phonon coupling (high CDW strength) to systems that are dominated by electron coupling between metal centers (low CDW strength).[1−5] The equitorial ligands, which lie perpendicular to the chain axis, are typically amine based, and all MX solids reported to date have identical ligands around each metal center. The chains themselves are weakly coupled to each other through hydrogen bonding on the amine ligands to the counterions between individual chains. These materials are model systems for the study of 1-D solids (including such 1-D systems as conjugated polymers) because of their chain like structure, their partial band filling, and the existence of polaronic defects.[6,7] Unlike most 1-D systems, which are often structurally inhomogeneous and have spectroscopic properties associated with (and in some cases dominated by) the distribution of polymer segments, MX solids form single crystals which are ordered along the 1-D chain axis (disordered from chain to chain). Even though MX chains are completely ordered within the chain axis, eliminating much of the structural inhomogeneity, the existence of polaronic defects, which give rise to sub-bandgap electronic states, can play a major role in the electronic and spectroscopic properties of these materials.[8,9]

The subject of this article is the structural and spectroscopic properties of a new MX solid; $[Pt(en)_2I_2][Pt(CN)_4]$. The purpose of the present contribution is to demonstrate that MX chains can be synthesized with varying ligand fields about alternating metal centers to yield systems in a nearly perfect mixed valent state {−Pt(II)−I−Pt(IV)−I−}. Because there are no counterions separating individual chains within $[Pt(en)_2I_2][Pt(CN)_4]$, we observe dramatically increased chain-to-chain interactions with respect to their charged counterparts. In fact this is the first report of a completely ordered (intrachain and interchain) MX material. All MX chains reported to date have displayed intense sub-bandgap absorptions. These absorptions have been assigned to transitions arising from intrinsic polaronic defects. $[Pt(en)_2I_2]$-$[Pt(CN)_4]$ displays no detectable sub-bandgap defects and is considered to be defect free (meaning free of polaronic defects). The combination of being a three-dimensionally ordered (structurally) single crystal and the absence of all defects giving rise to sub-bandgap states affords a unique opportunity to study the structural and spectroscopic properties of an extended 1-D material (electronically 1-D) without probing competing processes due to structural inhomogeneity or intrinsic defects.

Experimental Section

Synthesis. $[Pt(en)_2][Pt(CN)_4]$ was synthesized through the metathesis of stoichiometric amounts of $K_2[Pt(CN)_4]$ and [Pt-

* To whom correspondence should be addressed.
† University of New Mexico. Fax: 505-277-2609. E-mail: brozik@unm.edu.
‡ Los Alamos National Laboratory. Fax: 505-665-4631. E-mail: basil@lanl.gov.

10.1021/jp990460i CCC: $18.00
Published on Web 11/13/1999

$(en)_2]Cl_2$ in a minimum amount of deionized water. The resulting colorless crystals were collected, washed with cold deionized water, and dried in air. The starting materials, $K_2[Pt(CN)_4]$ and $[Pt(en)_2]Cl_2$, were purchased from Aldrich Chemical Co. and used as received. The MX chain, $[Pt(en)_2I_2][Pt(CN)_4]$, was prepared by first dissolving 1 mmol of $[Pt(en)_2][Pt(CN)_4]$ in warm deionized water followed by the slow dropwise addition of a solution of 0.5 mmol of I_2 dissolved in a minimum amount of ethanol. Upon addition of the I_2, a dark green precipitate formed. After complete addition, the mixture was diluted to 300 mL with deionized water and heated until all of the precipitate went into solution. Well formed single crystals of $[Pt(en)_2I_2][Pt(CN)_4]$ formed over a period of one week. The crystals possess a flat diamond shaped morphology and are highly reflective (silvery blue reflection).

Diffuse Reflectance. Because $[Pt(en)_2I_2][Pt(CN)_4]$ displays an intense axial polarized optical absorption,[20] it proved to be impossible to measure the optical absorption directly. As an alternative, we measured the diffuse reflectance spectrum with a Perkin-Elmer Lambda 19 UV−Vis−NIR spectrophotometer equipped with a Labsphere RSA-PE-19 dual beam diffuse reflectance attachment. The sample was prepared by dispersing 3 mg of $[Pt(en)_2I_2][Pt(CN)_4]$ in 300 mg of $MgSO_4$ by using a ball mill and sandwiching the resultant fine powder between two quartz plates separated by a 1.5 mm thick spacer. Pure $MgSO_4$, also ball milled into a fine powder, was used as a reference.

Resonance Raman. Samples for resonance Raman experiments were prepared by mounting a large single crystal on a specially designed mount and suspending it directly in liquid nitrogen inside a Pyrex optical dewar. To achieve wavelength-dependent spectra two separate excitation sources were utilized. For 800 nm excitation, a Coherent Innova 200I was used to pump a Coherent Mira-900 Ti:sapphire laser which was configured in cw mode. After attenuation, the beam intensity was 4 mW. A Quantronix Nd:YLF laser (in cw mode) was used to produce a 4 mW beam at 526 nm. The polarization was rotated with a half-wave plate polarization rotator to match the axially polarized IVCT band of the crystal. Resonance Raman scattering was monitored in a 180° backscattering configuration. The scattered light was dispersed with a Spex 1877 0.6 meter triple spectrometer, and detected with a liquid nitrogen cooled CCD camera (Princeton Instruments CCD-1152E/1).

Infrared Absorption. Samples for infrared absorption measurements were prepared by grinding a small amount of $[Pt(en)_2I_2][Pt(CN)_4]$ with Nujol to create an evenly dispersed mull. The Nujol mull was sandwiched between two matched KBr plates and mounted in a commercial FT-IR spectrometer (Bruker Equinox 55 FT-IR). A mid-IR spectrum was collected with a resolution of 2 cm^{-1}.

X-ray Crystallography. A dark, flat diamond shaped crystal was mounted on a glass fiber using five minute epoxy, and then placed on a Siemens P4/PC diffractometer. The radiation used was graphite monochromatized MoKα radiation ($\lambda = 0.71073$ Å). The lattice parameters were optimized from a least-squares calculation on 25 carefully centered reflections of high Bragg angle. The data were collected at room temperature using ω scans with a 0.90° scan range. Three check reflections monitored every 97 reflections showed no systematic variation in intensities. Lattice determination, data collection, and reduction, including Lorentz and polarization corrections, were carried out using XSCANS Version 2.10b software.[10] Structure solution, refinement, and graphics were performed using SHELXTL PC Version 4.2/360 software.[11] The data were corrected for absorption using the XEMP facility within SHELXTL PC. The structure was solved in space group *C*2/*m* using Patterson and difference Fourier techniques. This solution yielded all non-hydrogen atom positions. The methylene and amine hydrogen atoms were fixed in positions of ideal geometry, with C−H and N−H distances of 0.96 Å. The hydrogen atoms were refined using the riding model in the HFIX facility in SHELXL 93, with their isotropic temperature factors fixed at 1.2 times the equivalent isotropic U of the atom they were bonded to. Refinements in space groups *C*2 and *Cm* were not successful. The final refinement included anisotropic thermal parameters on all non-hydrogen atoms. Additional details of data collection and structure refinement are given in Table 1.

TABLE 1: Crystal Data and Structure Refinement for $[Pt(en)_2I_2][Pt(CN)_4]$

unit cell dimensions	$a = 10.577(1)$ Å $b = 11.595(1)$ Å; $\beta = 97.07°(1)$ $c = 7.253(1)$ Å
volume	882.75(17) Å^3
Z	2
density (calculated)	3.267 Mg/m^3
absorption coefficient	19.330 mm^{-1}
F(000)	764
crystal size	0.15 × 0.20 × 0.31 mm^3
Theta range for data collection	2.6 to 30.0°
Index ranges	$-1 \le h \le 14$, $-1 \le k \le 16$, $-10 \le l \le 10$
reflections collected	1684
independent reflections	1350 [R(int) = 0.0274]
completeness to theta = 30.00°	100.0%
refinement method	full-matrix least-squares on F^2
Data/restraints/parameters	1350/0/56
goodness-of-fit on F^2	1.045
final R indices [I>2sigma(I)]	R1* = 0.0269, wR2 = 0.0637
R indices (all data)	R1 = 0.0326, wR2 = 0.0661
extinction coefficient	0.00296(17)

*$R1 = \sum||F_o| - |F_c||/\sum|F_o|$ and $R2_w = [\sum[w(F_o^2 - F_c^2)^2]/\sum[w(F_o^2)^2]]^{1/2}$. The parameter $w = 1/[\sigma^2(F_o^2) + (0.0360P)^2]$.

Results

Structural Description. The crystals of the title compound crystallize in the monoclinic space group *C*2/*m*. The $[Pt(en)_2I_2]^{2+}$ and $[Pt(CN)_4]^-$ moieties both occupy sites of 2/*m* (C_{2h}) symmetry. In the $[Pt(en)_2I_2]^{2+}$ subunit the 2-fold axis bisects the C−C bonds of the en ligands. In the $[Pt(CN)_4]^{2-}$ subunit the 2-fold axis is coincident with one of the NC−Pt−CN axes. The structure of $[Pt(en)_2I_2][Pt(CN)_4]$ can in general be described as a kinked linear chain with a metal halide backbone of the sequence $-Pt^{2+}-I^-Pt^{4+}-I^-$ with the cyanide ligands attached to the Pt center of lower charge and the ethylenediamine ligands attached to the Pt center of higher charge (Figure 1). The chain itself is unique in that it has an overall neutral charge but has units of opposite but balancing charges within a single chain. Other MX chains have either neutral units within a chain or charge balance is achieved with counterions.

There are two points of particular interest. The first is the very strong dimerization of the bridging I^- sublattice. Of importance to one-dimensional solid-state materials is the degree of electron−phonon coupling which, in the case of MX solids, can manifest itself in terms of the charge disproportionation of the metal centers and the accompanying commensurate Peierls distortion of the halide sublattice (termed charge density wave or CDW). A good measure of the CDW strength is to observe experimentally the short to long Pt−I distance (ρ) which is typically $\rho = 0.9$ for platinum MX chains with iodide bridges.[12,13] In the present case, the value of $\rho = 0.789(1)$

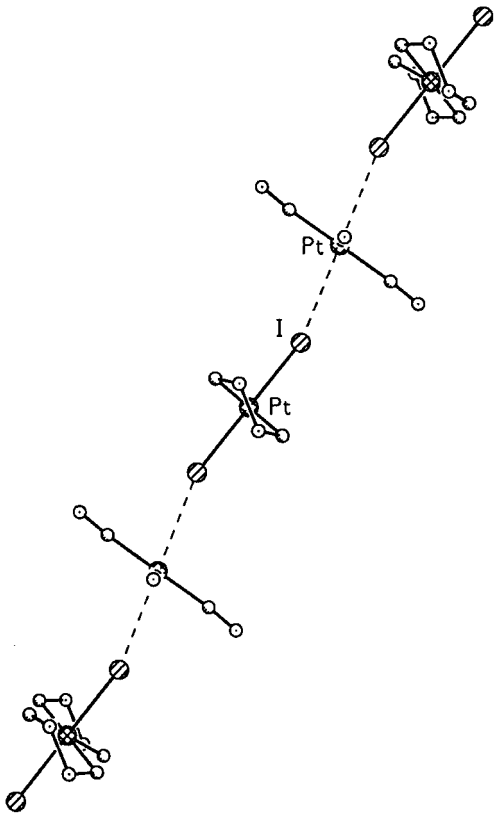

Figure 1. X-ray crystal structure of $[Pt(en)_2I_2][Pt(CN)_4]$ (en = ethylenediamine). The Pt atoms are coordinately bound to alternating en and CN^- ligands in a near square planar geometry, while the I^- ions connect the Pt sites along the chain.

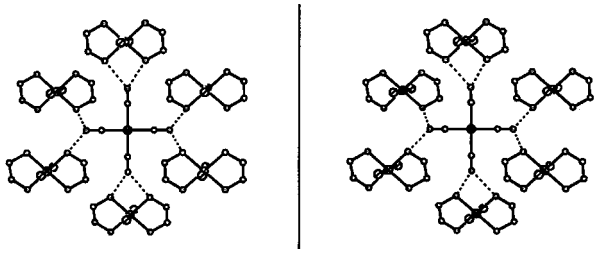

Figure 2. Packing arrangement of individual $[Pt(en)_2I_2][Pt(CN)_4]$ chains within the crystal. Each $Pt(II)(CN)_4$ subunit is surrounded by $Pt(IV)(en)_2$ subunits with short hydrogen-bonding distances between the nitrogen atoms on the CN^- ligands and the amine hydrogen atoms on the en ligand. The dashed lines show the CN···HN hydrogen bonding. (The hydrogen atoms have been omitted for clarity, and the dashed lines show the N(cyanide)−H(amine) contacts.)

makes $[Pt(en)_2I_2][Pt(CN)_4]$ the strongest CDW PtI material reported to date. This observation is consistent with the redox differences of the distinct Pt centers. Simply put, it is more difficult to oxidize $[Pt(CN)_4]^{2-}$ than $[Pt(en)_2]^{2-}$. Therefore, in addition to electron−phonon coupling, the redox differences of the Pt centers drive the charge disproportionation from the hypothetical symmetric −Pt(III)−I−Pt(III)−I− state to its charge disproportionated −Pt(II)−I−Pt(IV)−I− state. Furthermore, the platinum on the $[Pt(CN)_4]^{2-}$ subunit will possess the lower oxidation state.

The second point of interest is that $[Pt(en)_2I_2][Pt(CN)_4]$ is completely ordered (Figure 2). A general feature for all MX solids, except for the present case, is that the structures are disordered due to the fact that the chains are out of registry with respect to one another.[12] This results in two closely spaced electron density peaks in the bridging region. These peaks are usually centered between two adjacent Pt atoms and are related by a symmetry operation so that each peak has half occupancy. Such is not the case for $[Pt(en)_2I_2][Pt(CN)_4]$, which displays complete chain-to-chain registry. As will be discussed in detail below, a strong hydrogen-bonding network is setup between the nitrogen atoms on the tetracyanoplatinate units and the amine hydrogen atoms on the ethylenediamine ligands. The *N*(cyanide)−*N*(amine) distance in this hydrogen bond is 2.995 Å, which is at the lower end of reported N−H···N hydrogen bonds.[14] This hydrogen bonding is, in part, responsible for the observed chain-to-chain registry.

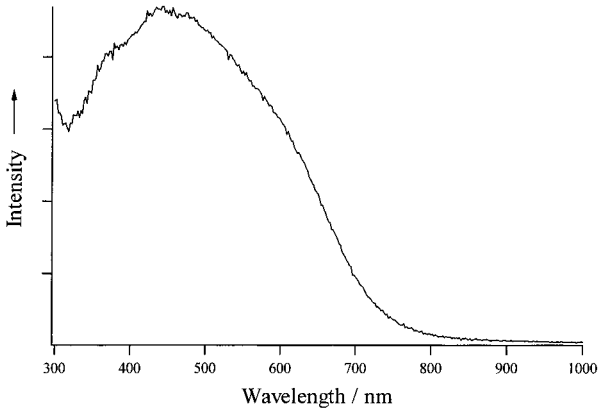

Figure 3. Diffuse reflectance spectrum of $[Pt(en)_2I_2][Pt(CN)_4]$ dispersed in $MgSO_2$.

TABLE 2: Infrared Data in the CN^- Stretching Region

compound	frequency (C≡N stretch)	assignment
$[Pt(en)_2I_2][Pt(CN)_4]$	2127 cm^{-1}; 2135 cm^{-1}	A_u; B_u (C_{2h} site symmetry)
$K_2[Pt(CN)_4]\cdot 3H_2O$[a]	2123 cm^{-1}; 2134 cm^{-1}	B_{2u}; B_{3u} (D_{2h} site symmetry)
$K_2[Pt(IV)(CN)_6]$[b]	2190 cm^{-1}	T_{1u} (O_h site symmetry)

[a] Reference 15. [b] Reference 16.

Diffuse Reflectance. The single crystals of $[Pt(en)_2I_2][Pt(CN)_4]$ possess an intense axially polarized absorption which has been assigned to an intervalence charge transfer band between adjacent platinum centers. Because of the intensity of the IVCT band, it proved to be impossible to measure the optical absorption along the chain axis directly. As an alternative, we measured the diffuse reflectance spectrum to achieve an approximation of the electronic absorption resulting in a low energy edge near 850 nm and peaking around 450 nm. The resulting diffuse reflectance data are plotted in Figure 3. Most noticeable is the complete absence of ground state sub-bandgap absorptions arising from ground state polaronic defects. All other MX solids display intense sub-bandgap signatures in their diffuse reflectance spectra, even with defect concentrations less than 1%.

Infrared Absorption in the CN Region. Because cyanide ligands back-bond with transition metals, measuring the CN stretching frequencies can report on the oxidation state of the platinum center containing the cyanide ligands. Listed in Table 2 is pertinent infrared data for $[Pt(en)_2I_2][Pt(CN)_4]$ along with relevant complexes containing CN^- ligands. The site symmetry of each chain in the lattice is C_{2h}; moreover, the site symmetry of each platinum center is also C_{2h}, giving rise to two distinct IR active CN stretches at 2127 and 2135 cm^{-1}, respectively. These frequencies are only marginally higher than the IR active CN stretching frequencies of $K_2[Pt(II)(CN)_4]\cdot 3(H_2O)$ {D_{2h} site symmetry with CN stretches at 2123 and 2134 cm^{-1}}[15] while

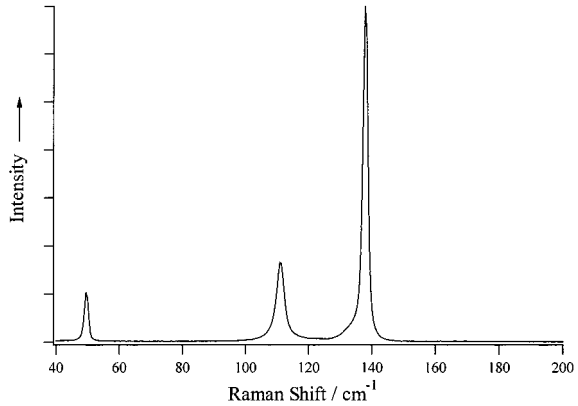

Figure 4. 77 K resonance Raman spectrum of a $[Pt(en)_2I_2][Pt(CN)_4]$ single crystal under 800 nm laser excitation (low frequency region).

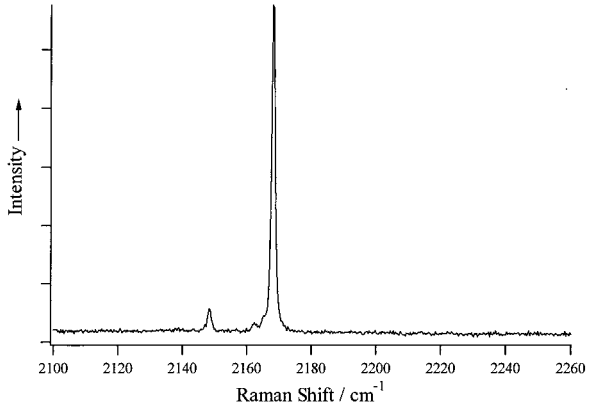

Figure 5. 77 K resonance Raman spectrum of a $[Pt(en)_2I_2][Pt(CN)_4]$ single crystal under 800 nm laser excitation (high frequency region).

$K_2[Pt(IV)(CN)_6]$ has a single strongly allowed IR active CN stretch {at 2190 cm^{-1}}[16] appearing much higher in energy. These results suggest that for the case of $[Pt(en)_2I_2][Pt(CN)_4]$ the oxidation state of the platinum center containing the cyanide ligands has an oxidation state close to that of Pt(II). This is in agreement with the I^- sublattice dimerizing around the platinum center containing the ethylenediamine ligands and the chain itself being highly charge disproportionated.

Resonance Raman. The results of resonance Raman experiments at 77 K with 800 nm excitation are depicted in Figures 4 and 5. Resonance Raman experiments at this excitation wavelength (which is in the tail of the IVCT absorption) reveal five strongly enhanced A_g modes at 49 cm^{-1} (ν_2), 111 cm^{-1} (ν_3), 138 cm^{-1} (ν_1), 2148 cm^{-1}, and 2168 cm^{-1}. It appears that these bands, especially, are highly coupled to the IVCT transition. The 2148 and 2168 cm^{-1} modes have been assigned to two A_g CN stretches (C_{2h} site symmetry) based on their similarity to the frequencies of $K_2[Pt(II)(CN)_4]\cdot(3\ H_2O)$ (2145 and 2165 cm^{-1} for the CN stretches respectively; D_{2h} point group symmetry)[15] and their Raman depolarization ratios.[19] Such close similarities in energy reiterate that the tetracyanoplatinate subunits in the chain are very nearly a Pt(II) center. Of particular significance is the observation that these modes are strongly enhanced upon 800 nm excitation. At this wavelength we are certainly not in resonance with any "molecular" states of the tetracyanoplatinate subunit where the lowest electronic transition is ~270 nm. This enhancement implies that the CN^- ligands are strongly coupled to the IVCT transition. This coupling can be understood by considering the strong π-back-bonding nature of the CN^- ligands. Through π-back-bonding interactions the vibrational frequencies of the CN^- ligands are strongly influenced by changes in electron density on the platinum, such as changes that occur during an IVCT transition.

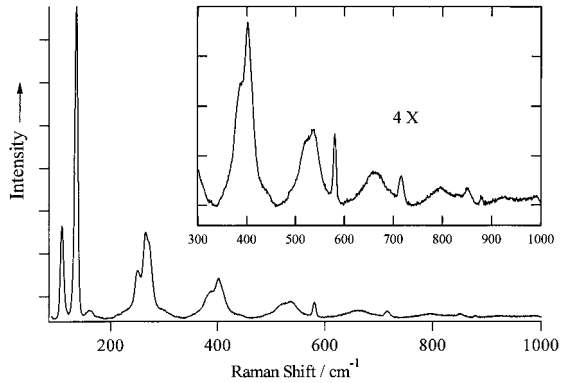

Figure 6. 77 K resonance Raman spectrum of a $[Pt(en)_2I_2][Pt(CN)_4]$ single crystal under 526 nm laser excitation (low frequency region).

TABLE 3: Resonance Raman Frequencies and Assignments

frequency (cm^{-1})	assignment[a]
110 (pk, vs)	ν_3
136 (pk, vs)	ν_1
160 (pk, w)	$\nu_2 + \nu_3$
250 (sh, s)	$\nu_3 + \nu_1$
265 (pk, vs)	$?_1$
272 (sh, vs)	$2\nu_1$
384 (sh, m)	$\nu_3 + 2\nu_1$
402 (pk, s)	$?_1 + \nu_1$
409 (sh, m)	$3\nu_1$
519 (sh, m)	$\nu_3 + 3\nu_1$
536 (pk, m)	$?_1 + 2\nu_1$
580.5 (pk, m)	Pt(IV)−N
716 (pk, w)	Pt(IV)−N + ν_1
852 (pk, w)	Pt(IV)−N + $2\nu_1$
988 (pk, vw)	Pt(IV)−N + $3\nu_1$

{ν_1, ν_2, and ν_3 are defined in the text; pk = peak, sh = shoulder, vs = very strong, s = strong, m = medium, w = weak, and vw = very weak; $?_1$ = unassigned}.

Of course the corollary of the tetracyanoplatinate subunit being nearly Pt(II), is that the bisethylenediamineplatinum subunit should be nearly Pt(IV). To that end we measured the symmetric I−Pt−I stretch of $[Pt(IV)(en)_2I_2]^{2+}$ in solution and found that its 140 cm^{-1} band matched closely the 138 cm^{-1} mode (ν_1) in $[Pt(en)_2I_2][Pt(CN)_4]$.[17] Because of this close correspondence we have assigned the 138 cm^{-1} mode to the symmetric A_g I−Pt−I stretch.[19] We were unable to find any molecular analogues for the strongly enhanced 49 and 111 cm^{-1} bands present in the title MX chain and must conclude that they are modes associated with the chain itself. (Note: It will be shown that these bands cannot arise from either factor group splitting or symmetry breaking due to site symmetry considerations; vide infra). Upon excitation deeper into the IVCT band at 526 nm, the appearance of a strong overtone progression along with combination bands is readily discernible (Figure 6). Assignments of the fundamentals, overtones, and combination bands for 526 nm excitation are listed in Table 3.

Discussion

Structure. The observed structure (and subsequent vibrational and diffuse reflectance measurements) clearly demonstrates the strong CDW nature of $[Pt(en)_2I_2][Pt(CN)_4]$. When CN^- ligands are coordinately bound to a metal, a π-bond is formed from a d(π) orbital on the metal into an antibonding 2p(π^*) orbital on

the ligand. The end result is that the platinum center on the $[Pt(CN)_4]^{2-}$ subunit is more difficult to oxidize than its $[Pt(en)_2]^{2+}$ counterpart. It is this difference in oxidation potential that drives $[Pt(IV)(en)_2I_2][Pt(II)(CN)_4]$ to its strong CDW state. The crystallization of the chain itself is easily understood by considering that the individual units are driven by charge neutralization between square planar $[Pt(II)(CN)_4]^{2-}$ and octahedral $[Pt(en)_2I_2]^{2+}$ subunits.

As mentioned in the results section, $[Pt(en)_2I_2][Pt(CN)_4]$ is the first MX solid to be completely ordered. Two crystalline forces drive the chain-to-chain registry. The crystal structure reveals a relatively short distance between the amine nitrogen atoms on the ethylenediamine ligands and the cyanide ligands on adjacent chains (vide supra, Figure 2). Moreover, the CN···HN hydrogen bond is the only one possible between $[Pt(en)_2I_2]^{2+}$ and $[Pt(CN)_4]^{2-}$ moieties. This highly specific and directional hydrogen bonding motif results in the chain-to-chain order observed in the crystal. This motif dictates that $[Pt(CN)_4]^{2-}$ subunits must be surrounded only by $[Pt(en)_2I_2]^{2+}$ subunits, and vice versa. Thus, there is no mechanism for disordering the chains with respect to each other. The second factor involved in the chain ordering is columbic interactions. Figure 2 shows that the registry between chains is such that each (−2) $Pt(CN)_4$ subunit is surrounded by six interchain (+2) $Pt(en)_2I_2$ subunits which results in charge neutralization between chains (as well as within a chain).

Electron and Phonon Structure. It is tempting to try to describe the electronic and vibrational nature of $[Pt(en)_2I_2][Pt(CN)_4]$ in terms of individual molecular units crystallizing in a unique structure and having localized molecular properties, especially when the ground state vibrational frequencies of the CN stretches and the symmetric I−Pt−I stretch is so close to those of the genuine Pt(II) and Pt(IV) molecular species, respectively. While easily articulated, such a simple molecular picture cannot fully account for the observed diffuse reflectance data in conjunction with the resonance Raman data. The axially polarized absorption can only be described in terms of an IVCT transition, which we have based on two facts. First the electronic spectra of the $[Pt(CN)_4]^{2-}$ and $[Pt(en)_2I_2]^{2+}$ are dissimilar in that their band edges (and absorption peaks) are much higher in energy than that observed for $[Pt(en)_2I_2][Pt(CN)_4]$ (band edges of $[Pt(CN)_4]^{2-}$(aq) and $[Pt(en)_2I_2]^{2+}$(aq) are at ∼290 nm and ∼690 nm, respectively).[17,18] Second, resonance Raman studies have shown a large enhancement of the modes associated with the symmetric I−Pt(IV)−I stretch and A_g CN modes at 800 nm excitation. We expect that both of these modes should report on electron density changes associated with individual platinum centers. Specifically, the symmetric I−Pt−I will report on changes associated with the $[Pt(en)_2I_2]^{2+}$ subunit and the A_g CN modes will report on changes associated with the $[Pt(CN)_4]^{2-}$ subunit. Since both are significantly enhanced, we conclude that at 800 nm (which is far from any "molecular states") that the electronic transition involves at least two adjacent Pt centers (and probably more). Because of the above-mentioned observations and reasoning and the apparent similarity to other MX chains, we have assigned the prominent axially polarized absorption to an IVCT transition and must conclude that the strong resonance enhancement is a result of strong electron−phonon coupling between the IVCT and the in-chain symmetric I−Pt−I stretch as well as the chain perpendicular A_g CN stretches.

There are two strongly enhanced Raman active vibrational modes, at 49 cm^{-1} (ν_2) and 111cm^{-1} (ν_3), which do not have any molecular counterparts. These modes must be the direct result either of factor group splitting, lowering of the symmetry of a subunit in the crystal lattice (site symmetry) to make an IR active mode Raman active, or as the result of chain formation. To determine this, we must consider the symmetry of the chain constrained within the crystal lattice. The space group has been determined to be *C*2/*m*. Let us first consider whether factor group splitting may play a role. Since there are two chain units passing through the crystallographic unit cell and two lattice points for the *C*2/*m* space group, the number of chain subunits within a Bravais cell is one. This result effectively excludes that these modes may arise from any factor group splitting. Next, consider if any IR active modes may become Raman active as a result of lowering the symmetry of a particular subunit due to its site symmetry within the crystal lattice. The factor group of the *C*2/*m* space group is isomorphic with the point group C_{2h}. Any particular chain within the unit cell has C_{2h} site symmetry. Therefore we need only consider the line group of any particular chain which is also isomorphic with the point group C_{2h}. The site symmetry of each Pt center within the line group is, once again, C_{2h}. Hence the inversion center is retained and therefore no IR modes become Raman active. Since there is no factor group splitting and the chain retains its inversion center, we conclude that the 49 and 111 cm^{-1} modes must arise from the formation of the chain itself.

Conclusion

In the above report we have described and characterized a new quasi-one-dimensional chain material. It has been demonstrated that this new material has a unique structure possessing complete chain-to-chain registry and order within each individual chain. The electronic properties can best be described in terms of an axially polarized intervalence charge transfer band between adjacent in-chain Pt(II) and Pt(IV) centers. The ground electronic state is highly charge disproportionated and nearly driven to a pure mixed valent configuration. The cause for this high CDW strength is the redox differences between individual platinum subunits as a result of their disparate ligand fields. This drives the CDW to a true mixed valent state in which the $[Pt(CN)_4]^{2-}$ subunit is very nearly Pt(II) and the $[Pt(en)I_2]^{2+}$ subunit is very nearly Pt(IV). Furthermore, the existence of resonance enhanced phonon modes associated with the chain, and not any particular molecular subunit, has led us to conclude that the phonon structure must be described through a more extended chain picture.

Acknowledgment. We gratefully acknowledge support by the Division of Material Science of the Office of Basic Energy Research at the DOE.

Supporting Information Available: Full details of the crystal and molecular structure determination is available free of charge via the Internet at http://pubs.acs.org.

References and Notes

(1) Scott, B.; Love, S. P.; Kanner, G. S.; Johnson, S. R.; Wilkerson, M. P.; Berky, M.; Swanson, B. I.; Saxena, A.; Huang, X. Z.; Bishop, A. R. *J. Mol. Struct.* **1995**, *356*, 207.

(2) Kuroda, N.; Sakai, M.; Nishina, Y.; Sasaki, K. *Phys. Rev. Lett.* **1992**, *68*, 3056.

(3) Interrante, L. V.; Browall, K. W. *Inorg. Chem.* **1974**, *5*, 1158.

(4) Miller, J. S.; Keller, H. J. *Extended Linear Chain Compounds*; Plenum: New York, 1992; Vol. 3, p 357.

(5) Toriumi, K.; Yoshiki, W.; Mitani, T.; Bandow, S. *J. Am. Chem. Soc.* **1989**, *111*, 2341.

(6) Baeriswyl, D.; Bishop, A. R. *Phys. Scr.* **1987**, *T19*, 239.

(7) Weber-Milbrodt, S. M.; Gammel, J. T.; Bishop, A. R.; Loh, E. Y. *Phys. Rev. B* **1992**, *45*, 6435.

(8) Kanner, G. S., Strouse, G. F.; Swanson, B. I. *Synth. Met.* **1997**, *86*, 1929.

(9) Kanner, G. S.; Strouse, G. F.; Swanson, B. I. *Phys. Rev. B* **1997**, *56*, 2501.

(10) XSCANS Version 2.10b, 1994, Siemens Analytical X-ray Incorporated: Madison, WI.

(11) SHELXTL Version 5.1, 1997, Siemens Analytical X-ray Incorporated: Madison, WI.

(12) Strouse, G. F.; Scott, B.; Swanson, B. I.; Saxena, A.; Batistic, I.; Gammel, J. T.; Bishop, A. R. *Chem. Phys. Lett.* **1998**, *289*, 559.

(13) Scott, B.; Berky, M.; Swanson, B. I. *Chem. Phys. Lett.* **1994**, *226*, 537.

(14) Pimentel, G. C.; McClellan, A. L. *The Hydrogen Bond* W. H. Freeman and Co.: San Francisco, 1960; p 288.

(15) Kubas, G. J.; Jones, L. H. *Inorg. Chem.* **1974**, *13*, 2816.

(16) Memering, M. M.; Jones, L. H.; Bailar, J. C. *Inorg. Chem.* **1973**, *12*, 2793.

(17) Brozik, J. A., unpublished results.

(18) Piepho, S. B.; Schatz, N. P.; McCaffery, A. J. *J. Am. Chem. Soc.* **1969**, *91*, 5994.

(19) Symmetry assignments of the Raman active 49 cm^{-1}, 111 cm^{-1}, 138, 2148, and 2168 cm^{-1} modes for $[Pt(en)_2I_2][Pt(CN)_4]$ as well as the 140 cm^{-1} mode in $[Pt(en)I_2]$ have been confirmed by measurement of Raman depolarization ratios.

(20) We were unable to perform single-crystal absorption studies, but were able to confirm the dichroic nature of an indexed crystal through the utilization of a polarization light microscope. White light perpendicular to the chain axis transmitted red light. White light polarized parallel to the chain axis did not transmit any visible radiation. From this result and in conjunction with similar results for other MX chains we have concluded that the axially polarized absorption is an IVCT.